

Adhesive stresses in axially-loaded tubular bonded joints - Part II: development of an explicit closed-form solution for the Lubkin and Reissner model

Original

Adhesive stresses in axially-loaded tubular bonded joints - Part II: development of an explicit closed-form solution for the Lubkin and Reissner model / Goglio, Luca; Paolino, Davide Salvatore. - In: INTERNATIONAL JOURNAL OF ADHESION AND ADHESIVES. - ISSN 0143-7496. - STAMPA. - 48:(2014), pp. 35-42. [10.1016/j.ijadhadh.2013.09.010]

Availability:

This version is available at: 11583/2515897 since:

Publisher:

Elsevier

Published

DOI:10.1016/j.ijadhadh.2013.09.010

Terms of use:

This article is made available under terms and conditions as specified in the corresponding bibliographic description in the repository

Publisher copyright

(Article begins on next page)

Please cite this article as:

“GOGGIO, L. and PAOLINO, D.S., 2014. Adhesive stresses in axially-loaded tubular bonded joints - Part II: Development of an explicit closed-form solution for the Lubkin and Reissner model. *International Journal of Adhesion and Adhesives*, **48**, pp. 35-42.”

**ADHESIVE STRESSES IN AXIALLY-LOADED TUBULAR BONDED JOINTS -
PART II: DEVELOPMENT OF AN EXPLICIT CLOSED-FORM SOLUTION FOR
THE LUBKIN AND REISSNER MODEL**

L. Goglio*, D.S. Paolino

Department of Mechanical and Aerospace Engineering, Politecnico di Torino, corso Duca degli Abruzzi 24, 10129 Torino, Italy

Abstract

The literature presents several analytical models and solutions for single- and double-lap bonded joints, whilst the joint between circular tubes is less common. For this geometry the pioneering model is that of Lubkin and Reissner (Trans. ASME 78, 1956), in which the tubes are treated as cylindrical thin shells subjected to membrane and bending loading, whilst the adhesive transmits shear and peel stresses which are a function of the axial coordinate only. Such assumptions are consistent with those usually adopted for the flat joints. A former investigation has shown that the L-R model agrees with FE results for many geometries and gives far better results than other models appeared later in the literature. The aim of the present work is to obtain and present an explicit closed-form solution, not reported by Lubkin and Reissner, which is achieved by solving the governing equations by means of the Laplace transform. The correctness of the findings, assessed by the comparison with the tabular results of Lubkin and Reissner, and the features of this solution are commented.

Keywords: C: Stress distribution; E: Joint design; Cylindrical joint.

*Corresponding author. Tel. +39 011 0906934; Fax: +39 011 0906999; E-mail: luca.goglio@polito.it

1. Introduction

The literature survey carried out in the first part of this study [1] and the related comparison with finite element (FE) results have evidenced that, among the known models of the tubular bonded joints under axial loading [2-9], only the one by Lubkin and Reissner [2] gives a truthful distribution of the peel stress in the overlap, while the shear component is predicted correctly in all models. Moreover, the FE results evidence that the peel and shear stresses are the most important components; the remaining ones, namely the axial and hoop stresses, have similar magnitude and are about one half of the peel stress.

On the basis of these findings, the aim of this work is reconsidering the model by Lubkin and Reissner to make up for its practical shortcoming, which is the lack of an explicit closed-form solution. The set of differential equations is solved by means of the Laplace transform, with a procedure modified to cope with the issue of dealing with a boundary problem (the known conditions are applied at the ends of the overlap) instead of an initial value problem (as in typical dynamic problems). The result is an explicit formula for the solution, which evidences the differences with respect to the flat lap joint and allows for direct calculation of the stresses.

2. Lubkin and Reissner model

The model by Lubkin and Reissner [2], for which a brief description has already been given in the first part [1] of the present study, is reviewed here in more detail. Figure 1 shows the shape of the joint as well as the geometrical and material properties.

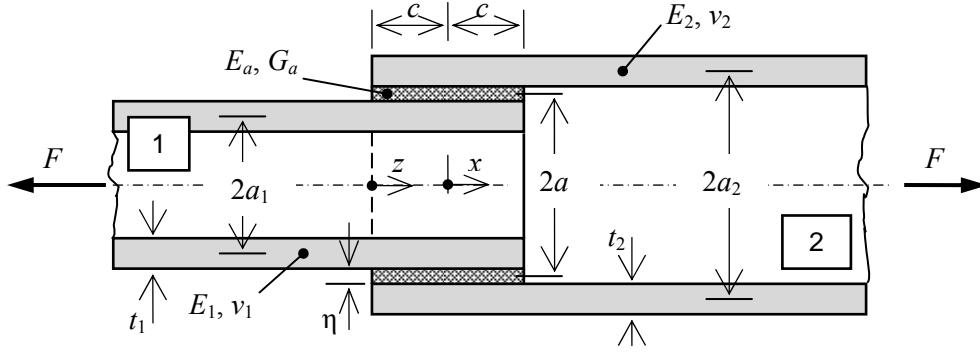


Fig. 1. Schematic of the tubular joint (also the related elastic constants are shown).

Considering first the tubes (subscripts 1, 2), a_1 and a_2 are the mean radii of the walls, E_1 and E_2 are the Young moduli, ν_1 and ν_2 are the Poisson's ratios. Regarding the adhesive (subscript a , when adopted), a is the mean radius of the layer, η is the thickness, E_a is the Young modulus, G_a is the shear modulus. The axial force loading the joint is F , the overlap length is $2c$; thus, having set the origin at midspan, the axial coordinate x varies in the range $\pm c$. Also the normalized coordinate z is adopted, varying between 0 (left end) and 1 (right end). With reference to Fig. 2, accounting for axial (T_1, T_2), transverse (V_1, V_2) and hoop (N_1, N_2) forces per unit length, bending moments (M_1, M_2) per unit length, peel (σ_y) and shear (τ_{xy}) stresses in the adhesive, the following equilibrium equations can be written for the two adherends:

$$a_1 \frac{dT_1}{dx} + a\tau_{xy} = 0 \quad a_2 \frac{dT_2}{dx} - a\tau_{xy} = 0 \quad (1a,b)$$

$$a_1 \frac{dV_1}{dx} + a\sigma_y - N_1 = 0 \quad a_2 \frac{dV_2}{dx} - a\sigma_y - N_2 = 0 \quad (2a,b)$$

$$a_1 \frac{dM_1}{dx} - a_1 V_1 + a \frac{t_1}{2} \tau_{xy} = 0 \quad a_2 \frac{dM_2}{dx} - a_2 V_2 + a \frac{t_2}{2} \tau_{xy} = 0 \quad (3a,b)$$

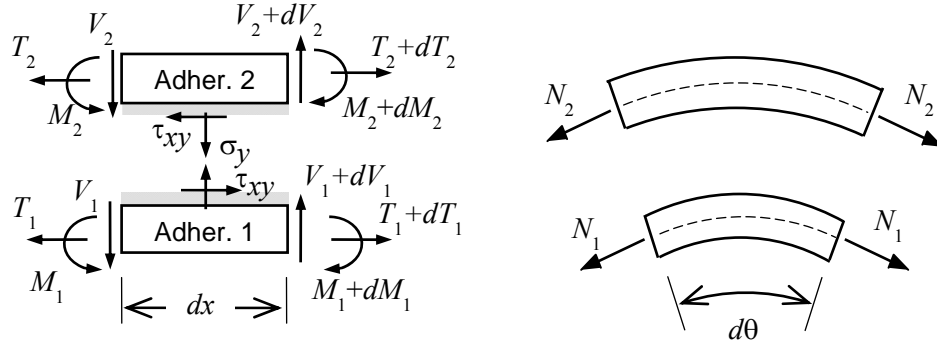


Fig. 2. Elementary free body diagrams for the joint.

The following equations of axial, hoop and bending deformability can be respectively written, which involve the longitudinal (u_1, u_2) and transverse (v_1, v_2) displacements at the mean radii of the tubes:

$$\frac{du_1}{dx} = \frac{T_1 - \nu_1 N_1}{E_1 t_1} \quad \frac{du_2}{dx} = \frac{T_2 - \nu_2 N_2}{E_2 t_2} \quad (4a,b)$$

$$\frac{v_1}{a_1} = \frac{N_1 - \nu_1 T_1}{E_1 t_1} \quad \frac{v_2}{a_2} = \frac{N_2 - \nu_2 T_2}{E_2 t_2} \quad (5a,b)$$

$$\frac{d^2 v_1}{dx^2} = -\frac{M_1}{D_1} \quad \frac{d^2 v_2}{dx^2} = -\frac{M_2}{D_2} \quad (6a,b)$$

where D_1, D_2 are the bending stiffnesses, defined as $D_i = E_i t_i^3 / 12(1 - \nu_i^2)$, with $i = 1, 2$.

The peel and shear stresses in the adhesive are related to displacements of the outer surface of tube 1 and inner surface of tube 2:

$$\sigma_y = \frac{E_a}{\eta} (v_2 - v_1) \quad (7)$$

$$\tau_{xy} = \frac{G_a}{\eta} (u_{2,in} - u_{1,ou}) \quad (8)$$

It must be noted that in equation (7) the surface displacements coincide with those of the mean surfaces, whilst in equation (8), accounting for the membrane and bending behaviour,

the displacements are $u_{1,ou} = u_1 - \frac{dv_1}{dx} \frac{t_1}{2}$ for the outer surface of tube 1 and $u_{2,in} = u_2 + \frac{dv_2}{dx} \frac{t_2}{2}$

for the inner surface of tube 2.

Thus, the problem involves in total fourteen equations –from (1a,b) to (6a,b), plus (7) and (8)– in the fourteen unknowns $T_1, V_1, N_1, M_1, u_1, v_1; T_2, V_2, N_2, M_2, u_2, v_2; \sigma_y, \tau_{xy}$, which are all a function of x . In the solution procedure depicted in [2], by means of a sequence of manipulation V_i, N_i, M_i, u_i ($i = 1,2$) and σ_y are eliminated; moreover, noticing that for the global axial equilibrium the condition $2\pi(a_1T_1 + a_2T_2) = F$ must hold, an auxiliary unknown T_0 is assumed such that

$$aT_0 = a_2T_2 - a_1T_1 \quad (9)$$

and, from equations (1a,b),

$$\frac{dT_0}{dx} = 2\tau_{xy} \quad (10)$$

Therefore, the axial forces per unit length T_1, T_2 and the shear stress in the adhesive τ_{xy} can be expressed as a function of such auxiliary unknown T_0 ; by mathematical manipulations a set of three simultaneous differential equations is obtained in the three unknowns v_1, v_2 and T_0 . Then, three dimensionless functions $g_1(z), g_2(z), g_3(z)$ are introduced, in which $z = (x + c)/2c$ is a dimensionless abscissa, such that:

$$v_1 = \frac{F}{2\pi a} \frac{(1-\nu_1^2)}{E_1} \left(\frac{2c}{t_1}\right)^2 g_1(z) \quad v_2 = \frac{F}{2\pi a} \frac{(1-\nu_2^2)}{E_2} \left(\frac{2c}{t_2}\right)^2 g_2(z) \quad T_0 = \frac{F}{2\pi a} g_3(z) \quad (11a,b,c)$$

The set of simultaneous differential equations becomes:

$$\begin{cases} g_1'' + (K_1^4 + \gamma_{11}^4)g_1 - \gamma_{12}^4 g_2 - \frac{3a}{a_1} g_3'' - \frac{3\Lambda_1 a}{a_1} g_3 = -\frac{3\Lambda_1 a}{a_1} \\ g_2'' + (K_2^4 + \gamma_{22}^4)g_2 - \gamma_{21}^4 g_1 - \frac{3a}{a_2} g_3'' + \frac{3\Lambda_2 a}{a_2} g_3 = -\frac{3\Lambda_2 a}{a_2} \\ g_3'' - \left(\frac{B_2^2}{a_2} + \frac{B_1^2}{a_1}\right) a g_3 - (B_2^2 g_2'' + B_1^2 g_1'') + \Lambda_2 B_2^2 g_2 - \Lambda_1 B_1^2 g_1 = \frac{B_2^2 a}{a_2} - \frac{B_1^2 a}{a_1} \end{cases} \quad (12a,b,c)$$

in which the primes indicate the differentiation order, and the coefficients $B_i, K_i, \Lambda_i, \gamma_{ij}$ ($ij =$

1,2) are defined as follows:

$$B_i^2 = (1 - \nu_i^2) \left(\frac{2c}{t_i} \right)^2 \frac{t_i G_a}{\eta E_i}, \quad K_i^4 = 12(1 - \nu_i^2) \left(\frac{2c}{t_i} \right)^4 \left(\frac{t_i}{a_i} \right)^2, \quad (13a,b)$$

$$\Lambda_i = 2\nu_i \left(\frac{2c}{t_i} \right)^2 \frac{t_i}{a_i}, \quad \gamma_{ij}^4 = 12(1 - \nu_j^2) \left(\frac{2c}{t_j} \right)^3 \frac{2c}{t_i} \frac{a E_a t_j}{a_i E_j \eta} \quad (13c,d)$$

The set of simultaneous equations (12) must be completed by the boundary conditions, according to the state at the ends of the overlap. It is evident that in the end sections of the tubes both axial and transverse forces are nil, as well as the bending moments; therefore $T_2 = V_2 = M_2 = 0$ in $x = -c$, $T_1 = V_1 = M_1 = 0$ in $x = c$. Conversely, in the sections where the overlap ends and the tubes continue as independent elements, the continuity of forces, moment, displacement and rotation must be ensured. Regarding this aspect, it can be recognized that in the tubes out of the overlap the bending behaviour is given by

$$v_1 = e^{\lambda_1 x} (A_{v1} \cos \lambda_1 x + B_{v1} \sin \lambda_1 x) - \frac{\nu_1 F}{2\pi E_1 t_1}, \quad v_2 = e^{-\lambda_2 x} (A_{v2} \cos \lambda_2 x + B_{v2} \sin \lambda_2 x) + \frac{\nu_2 F}{2\pi E_2 t_2} \quad (14a,b)$$

where $\lambda_i^4 = \frac{3(1 - \nu_i^2)}{a_i^2 t_i^2}$ and A_{vi}, B_{vi} ($i = 1,2$) are constants to be determined. This result can be

easily obtained by deleting the terms (related to the presence of the adhesive) which couple equations (12a) and (12b), or referring to the theory for bending of thin cylindrical shells (as can be found, e.g., in [10]).

Adopting the dimensionless abscissa (z) and functions (g_1, g_2, g_3), the set of boundary conditions, as reported in [1], in the left end of the overlap ($z = 0$) is

$$\begin{aligned}
g_{3_0} &= -1 \\
g_{2_0}'' &= 0 \\
g_{2_0}''' - \frac{3a}{a_2} g_{3_0}' &= 0 \\
g_{1_0}''' - \sqrt{2}K_1 g_{1_0}'' + K_1^2 g_{1_0}' - \frac{3a}{a_1} g_{3_0}' &= 0 \\
g_{1_0}'' - \sqrt{2}K_1 g_{1_0}' + K_1^2 g_{1_0} &= -2\sqrt{3} \nu_1 \frac{a}{a_1 \sqrt{1-\nu_1^2}}
\end{aligned} \tag{15}$$

and in the right end of the overlap ($z = 1$) is

$$\begin{aligned}
g_{3_1} &= 1 \\
g_{1_1}'' &= 0 \\
g_{1_1}''' - \frac{3a}{a_1} g_{3_1}' &= 0 \\
g_{2_1}''' + \sqrt{2}K_2 g_{2_1}'' + K_2^2 g_{2_1}' - \frac{3a}{a_2} g_{3_1}' &= 0 \\
g_{2_1}'' + \sqrt{2}K_2 g_{2_1}' + K_2^2 g_{2_1} &= -2\sqrt{3} \nu_2 \frac{a}{a_2 \sqrt{1-\nu_2^2}}
\end{aligned} \tag{16}$$

Note that in (15) and (16) the second subscript of the dimensionless functions stands for the value of z in which they are evaluated (0 or 1). The study of Lubkin and Reissner gives no additional details on the solution; it is only remarked that the equation set is linear with constant coefficients, thus “... *solution is possible by standard methods*”. The results reported in the paper are the normalized stress values (peel and shear) in 11 points of the overlap for a collection of 48 cases corresponding to different combinations of overlap length, stiffness and curvature.

3. Solution by means of the Laplace transform

In the search for an explicit closed-form solution of the problem, the major practical difficulty is given by the size, tenth order, of the set of differential equations. Although an approximate solution can be obtained without particular difficulties by numerical integration, the knowledge of the analytical form of the solution gives larger information and enables to

investigate the properties of solution, also by comparison with the case of the flat joint. The adopted procedure is based on the Laplace transform, which changes the equation set from differential to algebraic. By applying the transform to the simultaneous equations (12), the following set is obtained, here written in matrix form:

$$\begin{bmatrix} s^4 + K_1^4 + \gamma_{11}^4 & -\gamma_{12}^4 & -\frac{3a}{a_1}(s^2 + \Lambda_1) \\ -\gamma_{21}^4 & s^4 + K_2^4 + \gamma_{22}^4 & -\frac{3a}{a_2}(s^2 - \Lambda_2) \\ -B_1^2(s^2 + \Lambda_1) & -B_2^2(s^2 - \Lambda_2) & s^2 - \left(\frac{B_1^2}{a_1} + \frac{B_2^2}{a_2}\right)a \end{bmatrix} \begin{Bmatrix} G_1(s) \\ G_2(s) \\ G_3(s) \end{Bmatrix} = \frac{1}{s} \begin{Bmatrix} s^4 g_{1_0} + s^3 g_{1_0}' + s^2 \left(g_{1_0}'' - \frac{3a}{a_1} g_{3_0}' \right) + s \left(g_{1_0}''' - \frac{3a}{a_1} g_{3_0}'' \right) - \frac{3\Lambda_1 a}{a_1} \\ s^4 g_{2_0} + s^3 g_{2_0}' + s^2 \left(g_{2_0}'' - \frac{3a}{a_2} g_{3_0}' \right) + s \left(g_{2_0}''' - \frac{3a}{a_2} g_{3_0}'' \right) - \frac{3\Lambda_2 a}{a_2} \\ s^2 (g_{3_0} - B_1^2 g_{1_0} - B_2^2 g_{2_0}) + s (g_{3_0}' - B_1^2 g_{1_0}' - B_2^2 g_{2_0}') - \left(\frac{B_1^2 a}{a_1} - \frac{B_2^2 a}{a_2} \right) \end{Bmatrix} \quad (17)$$

in which s is the Laplacian complex variable and $G_1(s)$, $G_2(s)$, $G_3(s)$ are, respectively, the transforms of the functions $g_1(z)$, $g_2(z)$, $g_3(z)$.

The vector of the constant terms in the right hand side of the equation set (17) depends on g_1 , g_2 , g_3 and their derivatives calculated in $z=0$. By replacing the initial condition (15) in such vector, after several manipulations it is possible to obtain a vector of constant terms as a function of the initial conditions g_{1_0} , g_{1_0}' , g_{2_0} , g_{2_0}' , g_{3_0}' only. By solving the equation set (17), the Laplace transforms are obtained explicitly:

$$\begin{Bmatrix} G_1(s; g_{1_0}, g_{1_0}', g_{2_0}, g_{2_0}', g_{3_0}') \\ G_2(s; g_{1_0}, g_{1_0}', g_{2_0}, g_{2_0}', g_{3_0}') \\ G_3(s; g_{1_0}, g_{1_0}', g_{2_0}, g_{2_0}', g_{3_0}') \end{Bmatrix} = \frac{1}{s \cdot \sum_{i=0}^5 d_{2i} \cdot s^{2i}} \begin{Bmatrix} \sum_{i=0}^{10} n_{1,i} (g_{1_0}, g_{1_0}', g_{2_0}, g_{2_0}', g_{3_0}') \cdot s^i \\ \sum_{i=0}^{10} n_{2,i} (g_{1_0}, g_{1_0}', g_{2_0}, g_{2_0}', g_{3_0}') \cdot s^i \\ \sum_{i=0}^{10} n_{3,i} (g_{1_0}, g_{1_0}', g_{2_0}, g_{2_0}', g_{3_0}') \cdot s^i \end{Bmatrix} \quad (18)$$

In (18) the coefficients d_{2i} ($i = 0,1,\dots,5$) in the denominator are known, whilst the

coefficients $n_{1,i}$, $n_{2,i}$ and $n_{3,i}$ ($i = 0,1,\dots,10$) in the numerator are a function of the unknown initial conditions g_{1_0} , $g_{1_0}^I$, g_{2_0} , $g_{2_0}^I$ and $g_{3_0}^I$. Thus, it is worth of note that the Laplace transforms in (18) are rational functions which can be written as ratios of polynomials, of tenth degree in the numerator and of eleventh degree in the denominator. The polynomial in the denominator is the same for the three transforms and is obtained by the product of a bi-quintic polynomial, (i.e. a quintic polynomial in s^2) and the s variable; thus, it is immediate to recognize that $s=0$ is a root of the denominator. By decomposing in partial fractions the rational functions, an equivalent representation of the three Laplace transforms is obtained:

$$G_i(s; g_{1_0}, g_{1_0}^I, g_{2_0}, g_{2_0}^I, g_{3_0}^I) = \sum_{j=1}^{q+1} \sum_{k=1}^{Nm_j} \frac{C_{i,j,k}(g_{1_0}, g_{1_0}^I, g_{2_0}, g_{2_0}^I, g_{3_0}^I)}{(s-p_j)^{Nm_j-k+1}}, \quad i = 1,2,3, \quad (19)$$

in which q is the number of distinct roots (real or complex) of the bi-quintic polynomial, Nm_j is the algebraic multiplicity of the j -th root p_j , the coefficients (real or complex) $C_{i,j,k}$ are a function of the unknown initial conditions and are, according to the residue method for partial fractions decomposition (see e.g. [11]), equal to:

$$C_{i,j,k}(g_{1_0}, g_{1_0}^I, g_{2_0}, g_{2_0}^I, g_{3_0}^I) = \frac{1}{(k-1)!} \lim_{s \rightarrow p_j} \frac{d^{k-1}}{ds^{k-1}} \left[(s-p_j)^{Nm_j} G_i(s; g_{1_0}, g_{1_0}^I, g_{2_0}, g_{2_0}^I, g_{3_0}^I) \right] \quad (20)$$

In the numerous cases studied in this work, assuming for the elastic constants and the geometrical dimensions in (12) different values in a meaningful range of variation, the five roots obtained from the quintic polynomial in s^2 had always unit algebraic multiplicity; one of them was real and the remaining four were originated from two pairs of complex conjugates. The ten roots of the bi-quintic polynomial, easily obtainable from the five roots of the associated quintic polynomial, together with the trivial nil root can be finally expressed as:

$$\begin{aligned} p_1 = -p_6 = r_1 & & p_2 = -p_9 = r_2 + i \cdot m_2 & & p_3 = -p_{10} = r_3 + i \cdot m_3 \\ p_4 = -p_7 = r_2 - i \cdot m_2 & & p_5 = -p_8 = r_3 - i \cdot m_3 & & p_{11} = 0 \end{aligned}, \quad (21)$$

where r_1, r_2, r_3 and m_2, m_3 are respectively the absolute values of the real and imaginary parts different from zero (note that $m_1 = 0$) of the bi-quintic polynomial. It can be noticed that such roots can be easily obtained, starting from the quintic equation in s^2 , by finding numerically the only real root and calculating analytically (for the quartic polynomial explicit solutions for the roots are available) the two remaining pairs of complex conjugate roots.

Starting from the partial fractions decomposition (19) and considering the roots given in (21) it is possible to obtain the dimensionless functions $g_1(z), g_2(z), g_3(z)$ as a function of the initial unknown boundary conditions:

$$g_i(z; g_{1_0}, g_{1_0}^I, g_{2_0}, g_{2_0}^I, g_{3_0}, g_{3_0}^I) = \frac{n_{i,0}}{d_0} + \sum_{j=1}^{10} C_{i,j} e^{p_j z}, \quad i = 1, 2, 3, \quad (22)$$

where $n_{i,0}$ and d_0 are defined in Equation (18) and the coefficients $C_{i,j}$ are obtained from formula (20) by considering a unit algebraic multiplicity for each root (i.e., $Nm_j = 1$). In particular, the coefficients $C_{i,j}$ become equal to $\lim_{s \rightarrow p_j} (s - p_j) \cdot G_i(s; g_{1_0}, g_{1_0}^I, g_{2_0}, g_{2_0}^I, g_{3_0}, g_{3_0}^I)$.

Eventually, accounting for the definitions of the roots in (21) and through suitable manipulations, the explicit formulae for the dimensionless functions are obtained:

$$g_i(z; g_{1_0}, g_{1_0}^I, g_{2_0}, g_{2_0}^I, g_{3_0}, g_{3_0}^I) = \frac{n_{i,0}}{d_0} + \sum_{j=1}^3 \left(\cosh(r_j z) \cdot (c_{j,1,g_i} \cos(m_j z) + c_{j,2,g_i} \sin(m_j z)) + \sinh(r_j z) \cdot (c_{j,3,g_i} \cos(m_j z) + c_{j,4,g_i} \sin(m_j z)) \right), \quad i = 1, 2, 3 \quad (23)$$

in which the constants $c_{j,1,g_i}, c_{j,2,g_i}, c_{j,3,g_i}, c_{j,4,g_i}$ ($i, j = 1, 2, 3$) are real, depend on the unknown left ($z = 0$) conditions and are equal to

$$\begin{aligned} c_{1,1,g_i} &= C_{i,1} + C_{i,6} & c_{2,1,g_i} &= 2(\operatorname{Re}[C_{i,2}] + \operatorname{Re}[C_{i,7}]) & c_{3,1,g_i} &= 2(\operatorname{Re}[C_{i,3}] + \operatorname{Re}[C_{i,8}]) \\ c_{1,2,g_i} &= 0 & c_{2,2,g_i} &= -2(\operatorname{Im}[C_{i,2}] + \operatorname{Im}[C_{i,7}]) & c_{3,2,g_i} &= -2(\operatorname{Im}[C_{i,3}] + \operatorname{Im}[C_{i,8}]) \\ c_{1,3,g_i} &= C_{i,1} - C_{i,6} & c_{2,3,g_i} &= 2(\operatorname{Re}[C_{i,2}] - \operatorname{Re}[C_{i,7}]) & c_{3,3,g_i} &= 2(\operatorname{Re}[C_{i,3}] - \operatorname{Re}[C_{i,8}]) \\ c_{1,4,g_i} &= 0 & c_{2,4,g_i} &= -2(\operatorname{Im}[C_{i,2}] - \operatorname{Im}[C_{i,7}]) & c_{3,4,g_i} &= -2(\operatorname{Im}[C_{i,3}] - \operatorname{Im}[C_{i,8}]) \end{aligned} \quad i = 1, 2, 3 \quad (24)$$

where $\operatorname{Re}[\]$ and $\operatorname{Im}[\]$ indicate respectively the real and imaginary part of a complex number.

The dimensionless functions in (23) are still expressed as a function of the five unknown left conditions g_{1_0} , g'_{1_0} , g_{2_0} , g'_{2_0} and g'_{3_0} . Using the five right ($z=1$) boundary conditions given in (16), it is possible to build a set of algebraic equations which is linear (the unknown initial conditions appear always to the unit power) and easy to solve in the five unknowns g_{1_0} , g'_{1_0} , g_{2_0} , g'_{2_0} and g'_{3_0} . After this step, the three dimensionless functions $g_1(z)$, $g_2(z)$, $g_3(z)$ are completely determined and, therefore, it is possible to relate them to the peel and shear stresses in the adhesive by means of the equations (7), (10), (11) and (13a):

$$\begin{aligned}\sigma_y(z) &= \frac{F}{4\pi ac} \frac{E_a}{G_a} \left(B_2^2 \frac{2c}{t_2} g_2(z) - B_1^2 \frac{2c}{t_1} g_1(z) \right) \\ \tau_{xy}(z) &= \frac{F}{8\pi ac} g'_3(z)\end{aligned}\tag{25a,b}$$

Replacing in (25) the definitions (23) of the dimensionless functions and rearranging in suitable way the terms, the final formulae for the peel and shear stresses are obtained:

$$\begin{aligned}\sigma_y(z) &= \frac{F}{4\pi ac} \frac{E_a}{G_a} c_{0,\sigma} + \frac{F}{4\pi ac} \frac{E_a}{G_a} \sum_{i=1}^3 \left(\cosh(r_i z) \cdot (c_{i,1,\sigma} \cos(m_i z) + c_{i,2,\sigma} \sin(m_i z)) + \right. \\ &\quad \left. + \sinh(r_i z) \cdot (c_{i,3,\sigma} \cos(m_i z) + c_{i,4,\sigma} \sin(m_i z)) \right) \\ \tau_{xy}(z) &= \frac{F}{8\pi ac} \sum_{i=1}^3 \left(\cosh(r_i z) \cdot (c_{i,1,\tau} \cos(m_i z) + c_{i,2,\tau} \sin(m_i z)) + \right. \\ &\quad \left. + \sinh(r_i z) \cdot (c_{i,3,\tau} \cos(m_i z) + c_{i,4,\tau} \sin(m_i z)) \right)\end{aligned}\tag{26a,b}$$

where the new constants are given by

$$\begin{aligned}c_{0,\sigma} &= \frac{n_{2,0}}{d_0} B_2^2 \frac{2c}{t_2} - \frac{n_{1,0}}{d_0} B_1^2 \frac{2c}{t_1} \\ c_{i,j,\sigma} &= c_{i,j,g_2} B_2^2 \frac{2c}{t_2} - c_{i,j,g_1} B_1^2 \frac{2c}{t_1} \\ c_{i,1,\tau} &= r_i c_{i,3,g_3} + m_i c_{i,2,g_3} \\ c_{i,2,\tau} &= -(m_i c_{i,1,g_3} - r_i c_{i,4,g_3}) \\ c_{i,3,\tau} &= r_i c_{i,1,g_3} + m_i c_{i,4,g_3} \\ c_{i,4,\tau} &= -(m_i c_{i,3,g_3} - r_i c_{i,2,g_3})\end{aligned}\tag{27}$$

4. Numerical examples

To clarify the applicability of this procedure, the solution of two practical examples is shown in the following. For the first example the solution is presented step by step; for the second example, since the mathematical passages are the same, only the final equations are given in the text. The cases are taken from the collection reported in [2] and correspond to the examples 1 and 2 considered in [1]. In both cases, the two adherends have identical thickness and elastic constants, therefore $t_1 = t_2 = t$, $E_1 = E_2 = E$ and $\nu_1 = \nu_2 = 0.3$. The number of significant figures adopted in the following examples is chosen in order to show consistent numerical passages in the illustrative procedure and to obtain final results with the same numerical precision of the table of results reported in [2].

As for the first example, the other data, given in dimensionless form, are $E_a/G_a = 8/3$, $\beta = \eta E/(tE_a) = 20$, $2c/t = 10$, $R = t/(2a) = 0.025$. Considering such values and the boundary conditions in the left end ($z = 0$) the equation set (17) becomes

$$\begin{bmatrix} s^4 + 5887 & -5600 & -3.077s^2 - 9.468 \\ -5327 & s^4 + 5587 & -2.927s^2 + 8.566 \\ -1.706s^2 - 5.250 & -1.706s^2 + 4.994 & s^2 - 3.415 \end{bmatrix} \begin{Bmatrix} G_1(s) \\ G_2(s) \\ G_3(s) \end{Bmatrix} = \frac{1}{s} \begin{Bmatrix} s^4 g_{1_0} + s^3 g_{1_0}^I + s^2(-16.95g_{1_0} + 5.822g_{1_0}^I + 1.960) + s(-98.66g_{1_0} + 16.95g_{1_0}^I - 6.505) - 9.468 \\ s^4 g_{2_0} + s^3 g_{2_0}^I + 2.927s^2 - 8.566 \\ s^2(-1.706g_{1_0} - 1.706g_{2_0} - 1) + s(-1.706g_{1_0}^I - 1.706g_{2_0}^I + g_{3_0}^I) - 0.085 \end{Bmatrix}$$

The characteristic equation of the matrix is

$$s^{10} - 13.6578s^8 + 1.14709 \cdot 10^4 s^6 - 1.53928 \cdot 10^5 s^4 + 3.04267 \cdot 10^6 s^2 - 1.04739 \cdot 10^7 = 0$$

The real and imaginary parts of its roots are $r_1 = 2.00364$, $r_2 = 3.16908$, $r_3 = 7.27410$, $m_1 = 0$, $m_2 = 2.28471$, $m_3 = 7.27421$. As explained in the previous section, solving the above numerical equation set (corresponding to the equation set (17)) for $G_1(s)$, $G_2(s)$ and $G_3(s)$,

decomposing in partial fractions and inverse transforming, the dimensionless functions $g_1(z)$, $g_2(z)$, $g_3(z)$ are built, in which the coefficients still depend on the five unknown left conditions. Applying the five boundary conditions known in the right end the following linear equation set is written

$$\begin{bmatrix} -42.6495 & 13.3940 & -73.8104 & -8.24897 & 4.67366 \\ -39653.4 & 975.500 & 32490.4 & 736.253 & 11.3771 \\ -400526 & -34112.8 & 394177 & 32717.5 & 37.1474 \\ 621530 & 19318.7 & -563793 & -32492.3 & -88.5750 \\ 43783.5 & -4207.09 & -32708.4 & 802.598 & 26.8833 \end{bmatrix} \begin{Bmatrix} g_{1_0} \\ g_{1_0}^I \\ g_{2_0} \\ g_{2_0}^I \\ g_{3_0}^I \end{Bmatrix} = \begin{Bmatrix} 12.5090 \\ 525.747 \\ 1027.68 \\ -4673.17 \\ -768.563 \end{Bmatrix}$$

from which the five unknowns are obtained: $g_{1_0} = 0.00459$, $g_{1_0}^I = 0.02974$, $g_{2_0} = 0.02384$,

$g_{2_0}^I = -0.17159$, $g_{3_0}^I = 2.70675$. After this step, it is possible to calculate the coefficients (27)

to be replaced in the two formulae (26) so that the peel and shear stresses can be evaluated:

$$c_{0,\sigma} = -7.51960 \cdot 10^{-4};$$

$$\begin{array}{cccc} c_{1,1,\sigma} = 3.85793 \cdot 10^{-2} & c_{1,2,\sigma} = 0 & c_{1,3,\sigma} = -5.07453 \cdot 10^{-2} & c_{1,4,\sigma} = 0 \\ c_{2,1,\sigma} = -7.39931 \cdot 10^{-3} & c_{2,2,\sigma} = -1.29355 \cdot 10^{-3} & c_{2,3,\sigma} = 7.02210 \cdot 10^{-3} & c_{2,4,\sigma} = 1.91791 \cdot 10^{-3} ; \\ c_{3,1,\sigma} = 2.97887 \cdot 10^{-1} & c_{3,2,\sigma} = -1.63044 \cdot 10^{-1} & c_{3,3,\sigma} = -2.97874 \cdot 10^{-1} & c_{3,4,\sigma} = 1.63402 \cdot 10^{-1} \end{array}$$

$$\begin{array}{cccc} c_{1,1,\tau} = 3.82407 & c_{1,2,\tau} = 0 & c_{1,3,\tau} = -2.90724 & c_{1,4,\tau} = 0 \\ c_{2,1,\tau} = -1.12776 & c_{2,2,\tau} = -1.27933 & c_{2,3,\tau} = 1.11882 & c_{2,4,\tau} = 1.11739 \\ c_{3,1,\tau} = 1.04900 \cdot 10^{-2} & c_{3,2,\tau} = -8.33368 \cdot 10^{-3} & c_{3,3,\tau} = -1.04881 \cdot 10^{-2} & c_{3,4,\tau} = 8.31966 \cdot 10^{-3} . \end{array}$$

Adopting, as done in [1], the normalised stresses N (peel) and T (shear), respectively obtained dividing σ_y and τ_{xy} by $F/(4\pi ac)$, it is possible to plot the stress distribution in the joint independently of the intensity of the applied load. Figure 3 reports the graphs of N and T corresponding to the case under consideration, together with the relevant values published in [2]. As expected, the curves fit perfectly the points, since they are solutions of the same case.

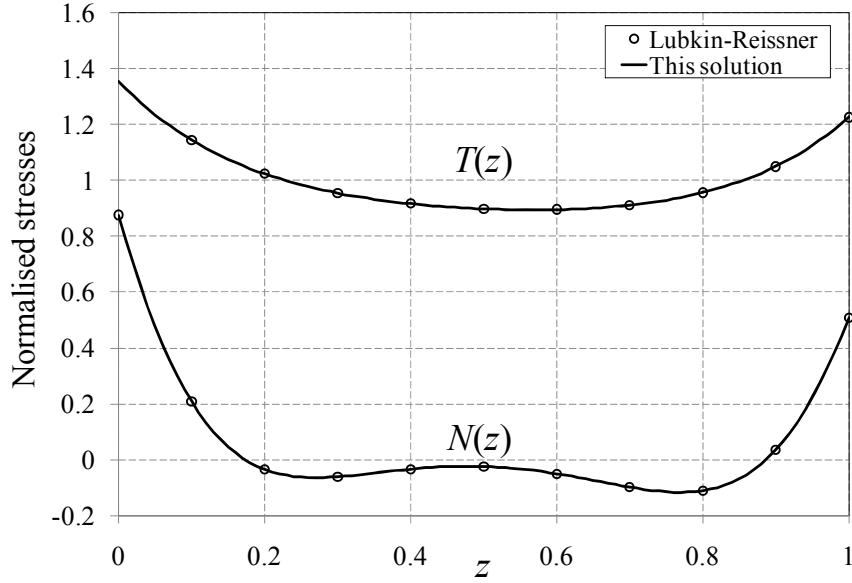


Fig. 3. Normalised stress distribution and comparison with the values published in [2], for the case $\beta = \eta E / (t E_a) = 20$, $2c/t = 10$, $R = t / (2a) = 0.025$.

As for the second example, the dimensionless data of the joint are $E_a/G_a = 8/3$, $\beta = 4$, $2c/t = 2$, $R = 0.1$. The chosen value for β corresponds to the one reported in the original tables given in [2]. However, as pointed out in [1], the results published in [2] correspond in reality to $\beta = 5$ rather than to $\beta = 4$. Indeed, by carrying out the analytical solution also in the $\beta = 5$ case, it will be shown in the following that data points given in [2] perfectly overlap the curve corresponding to $\beta = 5$.

For the $\beta = 4$ case, the real and imaginary parts are $r_1 = 0.97407$, $r_2 = 1.25917$, $r_3 = 2.21032$, $m_1 = 0$, $m_2 = 0.82959$, $m_3 = 2.20871$. The coefficients (27) to be replaced in the two formulae (26) so that the peel and shear stresses can be evaluated are:

$$c_{0,\sigma} = -2.27066 \cdot 10^{-3};$$

$$\begin{array}{cccc} c_{1,1,\sigma} = 4.28616 \cdot 10^{-2} & c_{1,2,\sigma} = 0 & c_{1,3,\sigma} = -9.27572 \cdot 10^{-2} & c_{1,4,\sigma} = 0 \\ c_{2,1,\sigma} = 1.18740 \cdot 10^{-3} & c_{2,2,\sigma} = -1.08671 \cdot 10^{-3} & c_{2,3,\sigma} = -1.45249 \cdot 10^{-3} & c_{2,4,\sigma} = 2.63564 \cdot 10^{-4} ; \\ c_{3,1,\sigma} = 2.48068 \cdot 10^{-1} & c_{3,2,\sigma} = -1.68834 \cdot 10^{-1} & c_{3,3,\sigma} = -3.14347 \cdot 10^{-1} & c_{3,4,\sigma} = 1.96836 \cdot 10^{-1} \end{array}$$

$$\begin{array}{cccc}
c_{1,1,\tau} = 5.15622 & c_{1,2,\tau} = 0 & c_{1,3,\tau} = -2.38261 & c_{1,4,\tau} = 0 \\
c_{2,1,\tau} = -2.89347 & c_{2,2,\tau} = -1.41093 & c_{2,3,\tau} = 1.49175 & c_{2,4,\tau} = 1.00293 \\
c_{3,1,\tau} = 6.19970 \cdot 10^{-2} & c_{3,2,\tau} = -3.29161 \cdot 10^{-2} & c_{3,3,\tau} = -4.99866 \cdot 10^{-2} & c_{3,4,\tau} = 2.65382 \cdot 10^{-2} .
\end{array}$$

For the $\beta = 5$ case, the real and imaginary parts are $r_1 = 0.81672$ $r_2 = 1.26293$ $r_3 = 2.10039$,

$m_1 = 0$, $m_2 = 0.911839$ $m_3 = 2.09897$. The coefficients (27) are:

$$c_{0,\sigma} = -2.22574 \cdot 10^{-3};$$

$$\begin{array}{cccc}
c_{1,1,\sigma} = 3.42099 \cdot 10^{-2} & c_{1,2,\sigma} = 0 & c_{1,3,\sigma} = -8.51426 \cdot 10^{-2} & c_{1,4,\sigma} = 0 \\
c_{2,1,\sigma} = 8.71122 \cdot 10^{-3} & c_{2,2,\sigma} = -3.92606 \cdot 10^{-3} & c_{2,3,\sigma} = -1.20372 \cdot 10^{-2} & c_{2,4,\sigma} = -1.11988 \cdot 10^{-3} ; \\
c_{3,1,\sigma} = 2.12117 \cdot 10^{-1} & c_{3,2,\sigma} = -1.38926 \cdot 10^{-1} & c_{3,3,\sigma} = -2.73003 \cdot 10^{-1} & c_{3,4,\sigma} = 1.73807 \cdot 10^{-1}
\end{array}$$

$$\begin{array}{cccc}
c_{1,1,\tau} = 3.89188 & c_{1,2,\tau} = 0 & c_{1,3,\tau} = -1.56374 & c_{1,4,\tau} = 0 \\
c_{2,1,\tau} = -1.68275 & c_{2,2,\tau} = -1.08036 & c_{2,3,\tau} = 7.74578 \cdot 10^{-1} & c_{2,4,\tau} = 9.12182 \cdot 10^{-1} \\
c_{3,1,\tau} = 5.38753 \cdot 10^{-2} & c_{3,2,\tau} = -2.91383 \cdot 10^{-2} & c_{3,3,\tau} = -4.29909 \cdot 10^{-2} & c_{3,4,\tau} = 2.15139 \cdot 10^{-2} .
\end{array}$$

Figure 4 reports the graphs of N and T corresponding to the cases under consideration (both $\beta = 4$ and $\beta = 5$), together with the relevant values published in [2] therein considered for $\beta = 4$. As anticipated, the data points given in [2] perfectly overlap only the curve corresponding to $\beta = 5$.

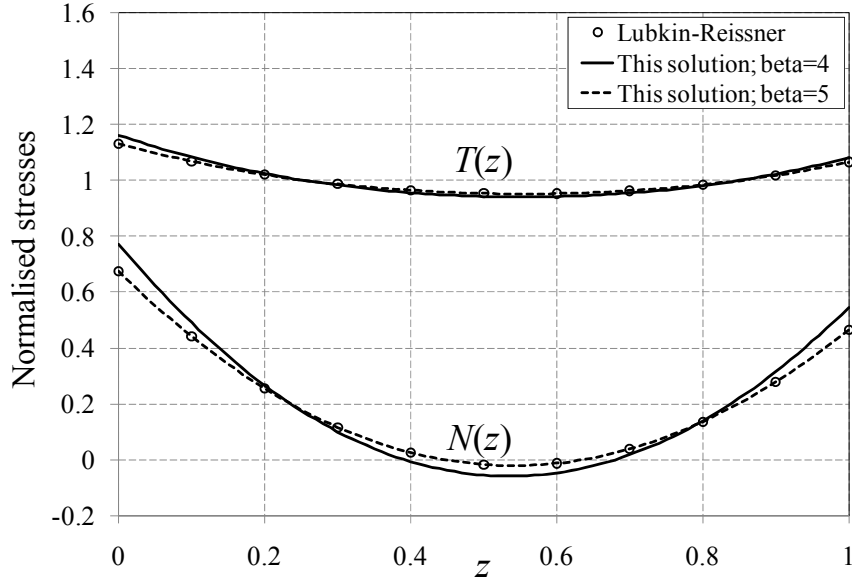


Fig. 4. Normalised stress distribution and comparison with the values published in [2], for the case $2c/t=2$, $R=t/(2a)=0.1$; data points for the case $\beta=\eta E/(tE_a)=4$, curves for the cases $\beta=4$ and $\beta=5$.

Every result given in [2] was accurately checked with the proposed analytical procedure: except for the results corresponding to $\beta=4$, the analytical solutions perfectly fit the data points. Results in [2] therein considered to values of $\beta=4$ were found to perfectly overlap the analytical solutions corresponding to $\beta=5$ in the present study. In this respect, in the tables given in [2], $\beta=4$ should be substituted by $\beta=5$.

6. Discussion

The closed-form solutions (26) obtained through the procedure described in this work exhibit the typical structure of the stress distributions for this class of problems, including hyperbolic terms ($m_1=0$), hyperbolic \times harmonic terms and, for the peel stress only, a constant term.

It can be useful to compare such solutions with those of the flat single lap joint, as found for

instance in [12]:

$$\begin{aligned}
\sigma_y(x) &= A_1 \cosh(p_1 x) + A_2 \sinh(p_1 x) + \\
&\quad + \cosh(q_1 x)(A_3 \cos(q_2 x) + A_4 \sin(q_2 x)) + \sinh(q_1 x)(A_5 \cos(q_2 x) + A_6 \sin(q_2 x)) \\
\tau_{xy}(x) &= B_1 \cosh(p_1 x) + B_2 \sinh(p_1 x) + \\
&\quad + \cosh(q_1 x)(B_3 \cos(q_2 x) + B_4 \sin(q_2 x)) + \sinh(q_1 x)(B_5 \cos(q_2 x) + B_6 \sin(q_2 x)) + B_7
\end{aligned} \tag{28a,b}$$

where A_1 - A_6 , B_1 - B_7 are constants to be determined from the boundary conditions, p_1 is the real root, q_1 and q_2 are respectively the real and imaginary parts of the complex roots. It is apparent that formulae (26) are characterized by the presence of a double number of hyperbolic-harmonic terms, due to the fact that the characteristic equation is bi-quintic instead of bi-cubic. Another difference is that the constant term appears in the peel stress for the tubular joints and in the shear stress for the flat joints. However, at least qualitatively, the distribution of the stresses, for the tubular and flat geometries is similar. The shear stress distribution exhibits the typical U-shape, which becomes flat as the overlap length becomes shorter. The peel stress distribution exhibits fluctuations in case of long overlap, tends to a U-shape when the overlap gets short.

Apart from this, there is no additional difficulty in implementing formulae (26a,b) in a spreadsheet, or in an house-made software, for stress calculation. As already remarked in [1], formulae based on the elastic approach are not suitable to predict the failure mode in detail, as this task requires the use of damage or fracture mechanics. However, the engineering usefulness of formulae like (26) or (28) is in the ease of building design tools, suitable to assess in quick manner the dimensions or the service load of bonded joints (as done, for instance, in [13] and [14]), a situation in which the assumption of elastic behaviour is acceptable. Another aspect of interest in the elastic formulae is in the fact that the obtained results can be regarded as the description of the “far field” stresses, upon which the analysis of the “local” stresses related to the edge singularity can be based (as tried in [15]).

7. Conclusions

Starting from a state-of-the-art review and FE results carried out in a companion paper, this work reconsidered the classical model by Lubkin and Reissner for the tubular joint under axial loading, and established a solution procedure based on the Laplace transform. The difficulty due to the fact that in this application the known conditions are given as boundary values, instead of initial values like in standard Laplace transforming, was overcome. The main achievement is that the solution is explicitly obtained in closed form, and contains more terms of hyperbolic \times harmonic type with respect to the case of the flat single lap joint.

The list of numerical results published by Lubkin and Reissner was compared to the results given by the obtained formulae. In general a perfect match was found, except for a systematic difference in a series of cases for which it was discovered that the value of the “elastothickness” parameter should be 5 instead of 4. The obtained formulae can be easily implemented in a spreadsheet or computer program to build a software tool for joint design.

References

- [1] L. Goglio, E. Dragoni. Adhesive stresses in axially-loaded tubular bonded joints – Part I: Critical review and finite element assessment of published models. *Int. J. Adhes. Adhes.* 2013;47:35-45.
- [2] J.L. Lubkin, E. Reissner. Stress distribution and design data for adhesive lap joints between circular tubes. *Trans. ASME* 1956;78:1213-1221.
- [3] Y.P. Shi, S. Cheng. Analysis of adhesive-bonded cylindrical lap joints subjected to axial load. *J. Eng. Mech.* 1993;119:584-602.
- [4] H. Nayeb-Hashemi, J.N. Rossettos, A.P.Melo. Multiaxial fatigue life evaluation of tubular adhesively bonded joints. *Int. J. Adhes. Adhes.* 1997;17:55-63.
- [5] N. Pugno, A. Carpinteri. Tubular adhesive joints under axial load. *J. Appl. Mech.* 2003;70:832-839.
- [6] O. Nemeş, F. Lachaud, A. Mojtabi. Contribution to the study of cylindrical adhesive joining. *Int. J. Adhes. Adhes.* 2006;26:474-480.
- [7] O. Nemeş, F. Lachaud. Modeling of cylindrical adhesively bonded joints. *J. Adhesion Sci. Technol.* 2009;23:1383-1393.
- [8] S. Kumar. Analysis of tubular adhesive joints with a functionally modulus graded bondline subjected to axial loads. *Int. J. Adhes. Adhes.* 2009;29:785-795.
- [9] S. Kumar, J.P. Scanlan. Stress analysis of shaft-tube bonded joints using a variational method. *J. Adhesion* 2010;86:369-394.
- [10] W.M. Coates. The state of stress in full heads of pressure vessels. *Trans. ASME* 1930;52:190-204.
- [11] S.T. Karris. Numerical analysis using MATLAB[®] and Excel[®], third ed., Orchard Publications, Fremont, 2007.
- [12] D.A. Bigwood, A.D. Crocombe. Elastic analysis and engineering design formulae for

bonded joints. *Int. J. Adhes. Adhes.* 1989;9:229-242.

[13] L.F.M. da Silva, R.F.T. Lima, R.M.S. Teixeira. Development of a computer program for the design of adhesive joints, *J Adhes.* 2009;85:889-918.

[14] E. Dragoni, L. Goglio, F. Kleiner. Designing bonded joints by means of the JointCalc software. *Int. J. Adhes. Adhes.* 2010;30:267-280.

[15] L. Goglio, M. Rossetto. Evaluation of the singular stresses in adhesive joints. *J. Adhesion Sci. Technol.* 2009;23:1441-1457.